Coulomb Excitation of Neutron-Rich Zn Isotopes: First Observation of the 2_1^+ State in ^{80}Zn

J. Van de Walle,[1,*] F. Aksouh,[1,2] F. Ames,[3] T. Behrens,[4] V. Bildstein,[4,5] A. Blazhev,[6] J. Cederkäll,[7] E. Clément,[7,2] T. E. Cocolios,[1] T. Davinson,[8] P. Delahaye,[7] J. Eberth,[6] A. Ekström,[9] D. V. Fedorov,[10] V. N. Fedosseev,[7] L. M. Fraile,[7] S. Franchoo,[7] R. Gernhauser,[4] G. Georgiev,[7,11] D. Habs,[3] K. Heyde,[12] G. Huber,[13] M. Huyse,[1] F. Ibrahim,[14] O. Ivanov,[1] J. Iwanicki,[15] J. Jolie,[6] O. Kester,[16] U. Köster,[17,7] T. Kröll,[4] R. Krücken,[4] M. Lauer,[5] A. F. Lisetskiy,[16,†] R. Lutter,[3] B. A. Marsh,[7] P. Mayet,[1] O. Niedermaier,[5] T. Nilsson,[16] M. Pantea,[18] O. Perru,[14] R. Raabe,[1] P. Reiter,[6] M. Sawicka,[1] H. Scheit,[5] G. Schrieder,[18] D. Schwalm,[5] M. D. Seliverstov,[13,10] T. Sieber,[7] G. Sletten,[19] N. Smirnova,[12,20] M. Stanoiu,[16] I. Stefanescu,[1] J.-C. Thomas,[1,21] J. J. Valiente-Dobón,[22] P. Van Duppen,[1] D. Verney,[14] D. Voulot,[7] N. Warr,[6] D. Weisshaar,[6] F. Wenander,[7] B. H. Wolf,[7] and M. Zielińska[15,2]

[1]*Instituut voor Kern- en Stralingsfysica, K.U. Leuven, Leuven, Belgium*
[2]*CEA Saclay, DAPNIA/SPhN, Gif-sur-Yvette, France*
[3]*Ludwig-Maximilians-Universität, München, Germany*
[4]*Physik Department E12, Technische Universität München, Garching, Germany*
[5]*Max-Planck-Institut für Kernphysik, Heidelberg, Germany*
[6]*Institut für Kernphysik, Universität Köln, Köln, Germany*
[7]*ISOLDE, CERN, Geneva, Switzerland*
[8]*University of Edinburgh, Edinburgh, United Kingdom*
[9]*Physics Department, University of Lund, Lund, Sweden*
[10]*Department of High Energy Physics, Petersburg Nuclear Physics Institute, Gatchina, Russia*
[11]*CSNSM, IN2P3-CNRS, Université Paris-Sud, Orsay, France*
[12]*Vakgroep Subatomaire en Stralingsfysica, Universiteit Gent, Gent, Belgium*
[13]*Institut für Physik, Johannes Gutenburg Universität Mainz, Mainz, Germany*
[14]*Institut de Physique Nucléaire, IN2P3-CNRS, Orsay, France*
[15]*Heavy Ion Laboratory, University of Warsaw, Warsaw, Poland*
[16]*Gesellschaft für Schwerionenforschung mbH, Darmstadt, Germany*
[17]*Institut Laue-Langevin, Grenoble, France*
[18]*Institut für Kernphysik, Technische Universität Darmstadt, Darmstadt, Germany*
[19]*Physics Department, University of Copenhagen, Denmark*
[20]*CENBG, CNRS/IN2P3, Université Bordeaux, Gradignan cedex, France*
[21]*GANIL, IN2P3-CNRS-CEA, Caen, France*
[22]*Instituto Nazionale di Fisica Nucleare, Laboratori Nazionali di Legnaro, Legnaro, Italy*

Neutron-rich, radioactive Zn isotopes were investigated at the Radioactive Ion Beam facility REX-ISOLDE (CERN) using low-energy Coulomb excitation. The energy of the 2_1^+ state in ^{78}Zn could be firmly established and for the first time the $2^+ \rightarrow 0_1^+$ transition in ^{80}Zn was observed at 1492(1) keV. $B(E2, 2_1^+ \rightarrow 0_1^+)$ values were extracted for ^{74,76,78,80}Zn and compared to large scale shell model calculations. With only two protons outside the $Z = 28$ proton core, ^{80}Zn is the lightest $N = 50$ isotone for which spectroscopic information has been obtained to date. Two sets of advanced shell model calculations reproduce the observed $B(E2)$ systematics. The results for $N = 50$ isotones indicate a good $N = 50$ shell closure and a strong $Z = 28$ proton core polarization. The new results serve as benchmarks to establish theoretical models, predicting the nuclear properties of the doubly magic nucleus ^{78}Ni.

Doubly magic nuclei form anchor points for our understanding of nuclear structure far from stability. Recent theoretical work has questioned the persistence of magic nucleon numbers, as we know them for stable nuclei, in nuclei with unusual neutron-to-proton (N/Z) ratios. Changes of the mean field potential or shifts of the effective single particle states have been suggested as possible causes [1,2]. In light nuclei, changing magic numbers have been confirmed experimentally [3,4], whereas for heavier nuclei indications have been observed [5]. A special class of nuclei are the neutron-rich isotopes around ^{78}Ni. The

$Z = 28$ shell closure is not a major harmonic oscillator shell closure but stems from the additional spin-orbit interaction. The weakening of this shell closure has been hinted by comparing recent experimental results with shell model (SM) calculations, utilizing an inert ^{48}Ca core [6,7]. It has been shown that due to the tensor part of the nucleon-nucleon interaction, the $Z = 28$ energy gap is strongly reduced when approaching the $N = 50$ closed shell [8]. With two protons outside the $Z = 28$ proton shell closure, $_{30}$Zn isotopes form an interesting set of nuclei to study the evolution of nuclear structure near the proton $Z = 28$ and

neutron $N = 50$ shell closures. In neutron-rich Zn isotopes ($A = 71$–80), neutrons occupy the SM $1g_{9/2}$ orbit, which separates the $N = 40$ subshell gap and the $N = 50$ shell gap. This unique parity neutron orbit in the 28 to 50 shell plays a distinctive role in the strength of the shell gaps and in the development of collectivity in this mass region, as evidenced by SM calculations compared to recently measured $B(E2)$ strengths in ^{70}Ni [7] and stable ^{64,66,68,70}Zn isotopes [9]. The increasing $B(E2)$ strengths in $^{70-74}$Zn [7,10] and the decreased $E(2_1^+)$ for $^{70-76}$Zn, as observed in β-decay studies of neutron-rich Cu isotopes [11], indicate increased collectivity in these neutron-rich Zn isotopes.

In this Letter we report on the measurement of $B(E2)$ values in ^{74,76,78,80}Zn and the determination of the 2_1^+ state in ^{78}Zn [half-life $T_{1/2} = 1.47(15)$ s] and ^{80}Zn [$T_{1/2} = 545(16)$ ms]. The latter is the lightest $N = 50$ isotone for which spectroscopic information becomes available. The reported results are compared to two large scale SM calculations.

The measurements, utilizing Coulomb excitation at sub-Coulomb barrier energies, were performed in 2004 ($A = 74, 76, 78$) and 2006 ($A = 80$) at the Radioactive Ion Beam (RIB) facility REX-ISOLDE (CERN) [12]. Low-energy Coulomb excitation is a very selective tool to establish the first excited 2^+ state in even-even isotopes, because of the dominating $E2$ excitation cross section.

The Zn beams were produced by bombarding a 50 g/cm^2 UC$_x$ target with 1.4 GeV protons with a maximum intensity of 3.2×10^{13} p/pulse at an average pulse repetition rate of 2.4 s. After diffusion out of the heated primary target, Zn isotopes were resonantly laser ionized [13], extracted, and mass separated. Due to the high temperature of the hot cavity, elements with a low ionization potential are surface ionized. The latter mechanism is the origin of strong contamination from Ga (all masses) and Rb ($A = 78, 80$) isotopes. During the $A = 78$ experiment, the proton beam was directed on a heavy metal rod (proton-to-neutron converter), which reduces the ^{78}Rb contamination considerably [14]. During the $A = 80$ experiment, a quartz tube was inserted in the transfer line, which absorbs alkaline elements such as Rb [15].

The mass separated RIB is accumulated, cooled, and bunched in a Penning Trap. Subsequently, the ion bunches are injected in an Electron Beam Ion Source at a rate of 12 Hz, where they are brought to high charge states. After an A/q separation ($q = 20^+$ for $A = 74, 76$ and $q = 21^+$ for $A = 78, 80$), the ions are post-accelerated by the REX linear accelerator [16] to a final energy of 2.87 MeV/nucleon ($A = 74, 78$), 2.83 MeV/nucleon ($A = 76$), and 2.79 MeV/nucleon ($A = 80$).

The post-accelerated beam was Coulomb excited on a 2.3 mg/cm^2 ^{120}Sn target ($A = 74, 76$) and a 2.0 mg/cm^2 ^{108}Pd target ($A = 78, 80$). The γ rays following the deexcitation process were detected by the MINIBALL

Germanium detector array [17], consisting of eight clusters, each containing three sixfold segmented HPGe crystals. The photopeak efficiency at 1 MeV after cluster addback is around 8.4%. The scattered beam and recoiling target particles were recorded in a 500 μm thick double sided silicon strip detector (DSSSD), consisting of four identical quadrants each containing 16 annular and 24 sector strips, covering laboratory angles between $\theta = 29°$–$52°$ ($A = 74, 76, 78$) and $\theta = 16.4°$–$52°$ ($A = 80$). Nuclei scattered in these angular ranges stem from collisions where the distance between the nuclear surfaces does not drop below 5 fm, ensuring that the observed excitation is induced by the electromagnetic interaction. The detected projectile nuclei could be kinematically separated from the recoiling target nuclei in the DSSSD. Because of the high segmentation of the experimental setup, the detected energy of the in-flight emitted γ rays can be corrected for its Doppler shift, utilizing the angular information on the γ ray and the detected projectile nucleus. Typical average beam intensities at the secondary target were 3.0×10^5 ($A = 74$), 1.1×10^5 ($A = 76$), 4.3×10^3 ($A = 78$), and 3.0×10^3 ($A = 80$) particles per second.

β-decay activity and room background in random coincidence with elastic scattered particles were subtracted from the prompt coincident γ spectra. The resulting random subtracted spectra are particularly clean of any background lines (see Fig. 1). All observed γ lines are due to Coulomb excitation of the target or beam nuclei.
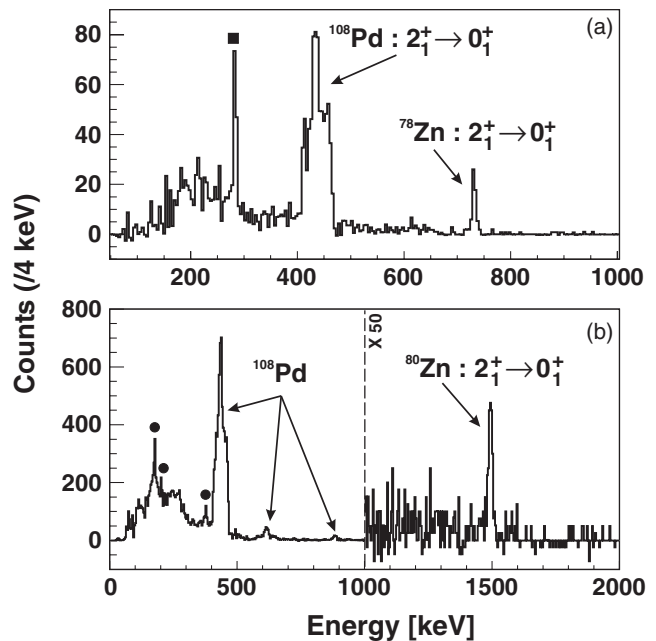

FIG. 1. Doppler corrected for the detected beam particle and random subtracted γ spectra during laser-ON periods, gated by detected ^{78}Zn, Ga (a) and ^{80}Zn, Ga, Rb (b) particles. The filled symbols indicate γ lines following Coulomb excitation of the dominant isobaric contaminants (circles = ^{80}Rb, square = ^{78}Ga).

Comparing γ-ray spectra accumulated with the lasers on and with the lasers off allowed us to discriminate between lines originating from the Coulomb excitation of Zn, isobaric contaminants and the target. Combining this information with literature [18], all γ lines in the laser-off spectra could be identified as Ga ($A = 74$–80) and Rb lines ($A = 80$). In ^{74,76}Zn, the $2_1^+ \rightarrow 0_1^+$ transition was known prior to our work (see Table I). The 730 keV line [see Fig. 1(a)], already observed in beta decay of ^{78}Cu and isomeric decay of ^{78}Zn, could be firmly established as the $2_1^+ \rightarrow 0_1^+$ transition in ^{78}Zn. The 1492 keV line [see Fig. 1(b)], only present in the laser-on spectrum obtained at mass 80, was identified as the $2_1^+ \rightarrow 0_1^+$ transition in ^{80}Zn.

The known $0_1^+ \rightarrow 2_1^+$ ($E2$) excitation cross section of the even-even target nucleus served as normalization to determine the excitation cross section of the Zn isotopes, which depends on the unknown $B(E2)$ value. The cross sections were deduced using the coupled channels Coulomb excitation code GOSIA [19], taking into account the angular distribution of the in-flight emitted γ rays, the energy loss of the beam in the target material, the position and relative efficiency of each MINIBALL cluster detector, and an integration over the angular range covered by the DSSSD. For ^{120}Sn and ^{108}Pd nuclei, adopted $B(E2)$ values [18,20,21] between all states involved in the excitation process were used in the calculation. The reorientation matrix element ($\langle 2_1^+ \| E2 \| 2_1^+ \rangle$), related to the spectroscopic quadrupole moment of the 2_1^+ state was fixed to 0.0 eb in all Zn isotopes. The influence of the unknown $\langle 4_1^+ \| E2 \| 2_1^+ \rangle$ on the resulting $\langle 2_1^+ \| E2 \| 0_1^+ \rangle$, assuming a vibrational $B(E2, 4_1^+ \rightarrow 2_1^+)$, is in all cases below 0.5%.

Isobaric beam contamination, which can strongly influence the normalization to the target excitation, was determined using different methods. An analysis of the radioactivity measured with MINIBALL at the target station revealed that the $A = 74$, 76, 78 Zn beam was only contaminated with Ga. For mass $A = 80$, also a Rb contamination was observed. From the γ-line intensity and known branching ratios [18], the beam composition was deduced. Additionally, the ratio of laser (Zn) over surface ionized (Ga,Rb) beam particles was determined by switching the laser ionization periodically on and off. The ratio was extracted from the difference in elastic scattering in

the DSSSD and the induced target excitation. Both methods yield a consistent ratio. In the laser-on periods, decay losses of ^{80}Zn during the average trapping time (maximum 78 ms) and constant charge breeding time (78 ms) were taken into account. These corrections are negligible for ^{74,76,78}Zn due to their relatively long half-life. The composition of the $A = 78$ RIB was checked with a ΔE-E gas-Si telescope placed at the end of the REX linear accelerator, confirming that the only contaminant is ^{78}Ga (see Ref. [14]). The deduced Zn content in the isobaric RIB's is : 83(4)% ($A = 74$), 73(7)% ($A = 76$), 64(13)% ($A = 78$), and 43(5)% ($A = 80$).

The resulting $E(2_1^+)$ and $B(E2)$ values are summarized in Table I. The error on the $B(E2)$ is dominated by the statistical error on the number of counts in the $2_1^+ \rightarrow 0_1^+$ transitions and the uncertainty on the beam composition. Our measurement is in good agreement with the recently measured $B(E2)$ value for ^{74}Zn [7]).

In Fig. 2 the $E(2_1^+)$ and $B(E2)$ systematics for even-even Ni, Zn, and Ge isotopes are compared. In Fig. 3, the same systematics for $N = 50$ isotones is shown. In both figures, two sets of SM calculations are included for Zn isotopes and $N = 50$ isotones.

The $E(2_1^+)$ and $B(E2)$ systematics around ^{78}Ni is dominated by the $Z = 28$ and $N = 50$ shell closures and the $N = 40$ subshell closure. The $B(E2)$ systematics around $N = 40$ (^{68,70}Ni [7,22] and ^{72,74}Zn [7,10]) is determined by the filling of the unique parity $\nu 1g_{9/2}$ orbit and the $Z = 28$ proton core polarization. The strongly decreasing $B(E2)$ trend for neutron-rich Zn isotopes ($N > 42$) is similar to the systematics observed in Ge (see Fig. 2) and Se isotopes
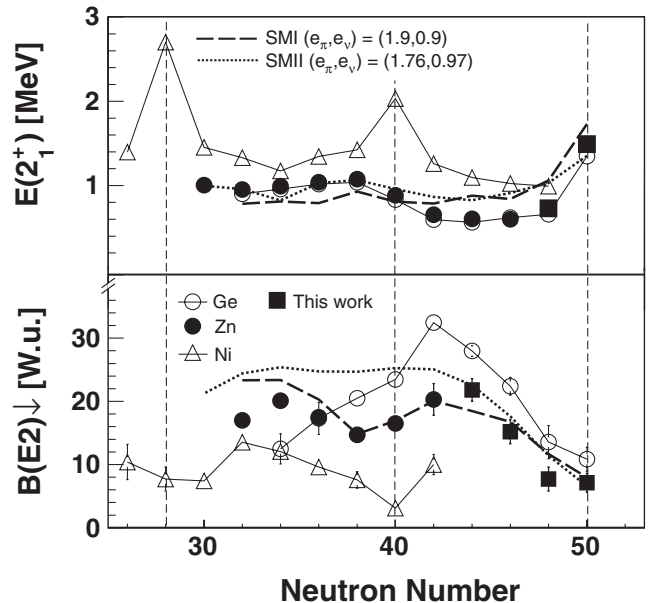
TABLE I.   Experimental (exp) and calculated (SMI and SMII) $E(2_1^+)$ and $B(E2)$ values for ^{74,76,78,80}Zn (see text for the difference between SMI and SMII).

	$E_{2_1^+}$ [keV]			$B(E2)\uparrow [(eb)^2]$		
	exp	SMI	SMII	exp	SMI	SMII
^{74}Zn	606	879	782	0.201(16)	0.171	0.209
^{76}Zn	599	840	826	0.145(18)	0.161	0.169
^{78}Zn	730[a]	1060	924	0.077(19)	0.116	0.113
^{80}Zn	1492(1)[a]	1731	1353	0.073(15)	0.082	0.067

[a]newly established 2_1^+ state.

FIG. 2. $E(2_1^+)$ and $B(E2)\downarrow$ systematics for Ni ($Z = 28$), Zn ($Z = 30$), and Ge ($Z = 32$) isotopes. $B(E2)\downarrow$ values were taken from Refs. [6,7,9,10,18,30]. The dashed and dotted lines correspond to SM calculations for Zn isotopes.
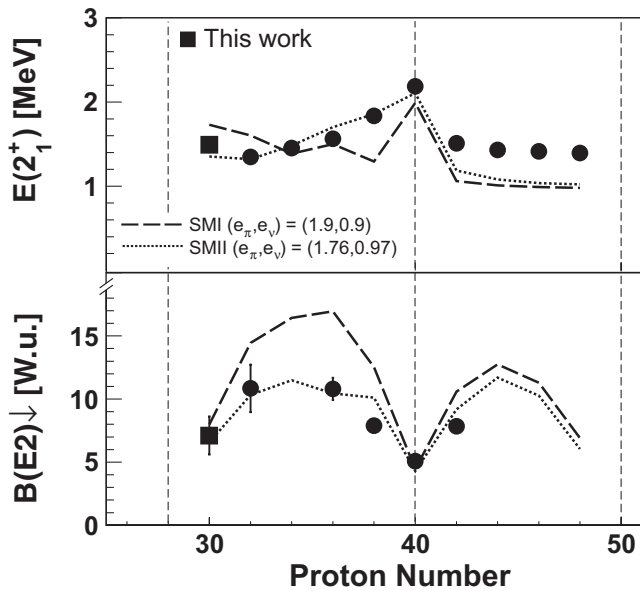
FIG. 3. $E(2_1^+)$ and $B(E2)$ values for $N = 50$ isotones. The dashed and dotted lines correspond to SM calculations.

(not shown) and hints at a strong $N = 50$ neutron shell closure.

The first set of SM calculations (labeled SMI) utilizes the realistic effective nucleon-nucleon interaction based on G-matrix theory by Hjorth-Jensen [23], with the monopole modification by Nowacki [24,25]. The model space consists of proton/neutron $2p_{3/2}$, $1f_{5/2}$, $2p_{1/2}$, and $1g_{9/2}$ orbits around an inert ^{56}Ni core. High π/ν effective charges of $1.9e/0.9e$ were used to compensate for the large ^{56}Ni core polarization, since SM and Monte Carlo SM calculations show that the doubly closed shell probability of ^{56}Ni is only $\sim$65% [26] and $\sim$50% [27]. The second set of SM results (SMII) were obtained with the JJ4B effective interaction [28] which is an extension of the renormalized G-matrix interaction based on the Bonn-C NN potential (JJ4APN) constructed to reproduce the experimental data for exotic Ni, Cu, Zn, Ge, and $N = 50$ isotones in the vicinity of ^{78}Ni. π/ν polarization charges of $1.76e$ and $0.97e$ were used, which reproduce known $B(E2, 8_1^+ \rightarrow 6_1^+)$ values in ^{92}Mo (e_π) and ^{70}Ni (e_ν).

Both SM calculations reproduce the $B(E2)$ trend in the Zn isotopic chain. Around $N = 40$, the SMII results are sensitive to the position of the excited 0_2^+ state. A similar problem in the Ge isotopes has been discussed in Ref. [29].

The calculated $B(E2)$ strength for the $N = 50$ isotones is solely due to proton excitations, since neutron excitation across the $N = 50$ gap are not included in the valence space. The SMI results overestimate the $B(E2)$ strengths in Ge ($Z = 32$), Kr ($Z = 36$), and Sr ($Z = 38$), whereas the new ^{80}Zn result is reproduced. Reducing the e_π in SMI would reproduce the Ge, Kr, and Sr results but conflict with the ^{80}Zn result, where a large e_π is still needed. The empirically adapted π-π effective interaction, contained

in JJ4B, reproduces well the $N = 50$ systematics (see Fig. 3), indicating the persistence of the $N = 50$ shell gap down to $Z = 30$. The need for a high e_π in both SMI ($e_\pi = 1.9e$) and SMII ($e_\pi = 1.76e$) in order to reproduce the ^{80}Zn result indicates a strong $Z = 28$ core polarization.

In conclusion, Coulomb excitation experiments on neutron-rich Zn isotopes at "safe" energies using post-accelerated radioactive ion beams have been performed and the 2_1^+ energy and $B(E2)$ systematics has been extended up to $N = 50$. Data on ^{80}Zn, only two protons away from ^{78}Ni, have been obtained. SM calculations of the $N = 50$ isotones, assuming only protons as the active valence particles, are in good agreement with the experimental results, provided the use of a large e_π. This indicates a good $N = 50$ shell closure and strong $Z = 28$ core polarization around ^{78}Ni.

*Present address: ISOLDE, CERN, Geneva, Switzerland.
†Present address: University of Arizona, Tucson, Arizona, USA.
[1] J. Dobaczewski *et al.*, Phys. Rev. Lett. **72**, 981 (1994).
[2] T. Otsuka *et al.*, Phys. Rev. Lett. **87**, 082502 (2001).
[3] A. Ozawa *et al.*, Phys. Rev. Lett. **84**, 5493 (2000).
[4] J. Fridmann *et al.*, Phys. Rev. C **74**, 034313 (2006).
[5] I. Dillmann *et al.*, Phys. Rev. Lett. **91**, 162503 (2003).
[6] J. Leske *et al.*, Phys. Rev. C **71**, 034303 (2005).
[7] O. Perru *et al.*, Phys. Rev. Lett. **96**, 232501 (2006).
[8] T. Otsuka *et al.*, Phys. Rev. Lett. **97**, 162501 (2006).
[9] O. Kenn *et al.*, Phys. Rev. C **65**, 034308 (2002).
[10] S. Leenhardt *et al.*, Eur. Phys. J. A **14**, 1 (2002).
[11] J. Van Roosbroeck *et al.*, Phys. Rev. C **71**, 054307 (2005).
[12] D. Habs *et al.*, Hyperfine Interact. **129**, 43 (2000).
[13] V. Fedoseyev *et al.*, Hyperfine Interact. **127**, 409 (2000).
[14] U. Köster *et al.*, AIP Conf. Proc. **798**, 315 (2005).
[15] E. Bouquerel *et al.*, Eur. Phys. J. A (to be published).
[16] O. Kester *et al.*, Nucl. Instrum. Methods Phys. Res., Sect. B **204**, 20 (2003).
[17] J. Eberth *et al.*, Prog. Part. Nucl. Phys. **46**, 389 (2001).
[18] URL http://www.nndc.bnl.gov/nndc/nudat/.
[19] T. Czosnyka *et al.*, Bull. Am. Phys. Soc. **28**, 745 (1983).
[20] S. Raman, At. Data Nucl. Data Tables **78**, 1 (2001).
[21] L. Svensson *et al.*, Nucl. Phys. A **584**, 547 (1995).
[22] O. Sorlin *et al.*, Phys. Rev. Lett. **88**, 092501 (2002).
[23] M. Hjorth-Jensen *et al.*, Phys. Rep. **261**, 125 (1995).
[24] F. Nowacki, Ph.D. thesis, IReS, Strasbourg, 1996.
[25] N. Smirnova *et al.*, Phys. Rev. C **69**, 044306 (2004).
[26] M. Honma *et al.*, Phys. Rev. C **69**, 034335 (2004).
[27] T. Otsuka *et al.*, Phys. Rev. Lett. **81**, 1588 (1998).
[28] A. Lisetskiy *et al.*, Phys. Rev. C **70**, 044314 (2004).
[29] M. Hasegawa *et al.*, Nucl. Phys. A (to be published).
[30] E. Padilla-Rodal *et al.*, Phys. Rev. Lett. **94**, 122501 (2005).